Model Following Sliding-Mode Control of a Six-Phase Induction Motor Drive

Navid R. Abjadi[†], Gholamreza Arab Markadeh[*], and Jafar Soltani[**]

[†][*] Dept. of Eng., Shahrekord University, Shahrekord, Iran
[**] Dept. of Electrical and Computer Eng., Isfahan University of Technology, Isfahan, Iran
[**] Dept. of Eng., Islamic Azad University – Khomeinishahr Branch, Khomeinishahr, Iran

Abstract

In this paper an effective direct torque control (DTC) and stator flux control is developed for a quasi six-phase induction motor (QIM) drive with sinusoidally distributed windings. Combining sliding-mode (SM) control and adaptive input-output feedback linearization, a nonlinear controller is designed in the stationary reference frame, which is capable of tracking control of the stator flux and torque independently. The motor controllers are designed in order to track a desired second order linear reference model in spite of motor resistances mismatching. The effectiveness and capability of the proposed method is shown by practical results obtained for a QIM supplied from a voltage source inverter (VSI).

Key Words: Model-following, Multiphase machines, Sliding-mode control

I. INTRODUCTION

Recently the use of multiphase machines in various industrial applications especially ones that require more than one electric motor drive such as electric vehicles, textiles, web processing and paper mills has been increasing. The advantages of multiphase machines are their higher torque density, higher efficiency, reduced torque pulsations, greater fault tolerant, improved drive noise characteristic, and a reduction in the required rating per inverter, leg all of which result in simpler and more reliable power conditioning equipment [1]-[7].

Recently, multi-level inverters have been used in many industrial applications [8], [9], in fact multi-phase inverters are the dual of multi-level inverters.

Adjustable speed drives (ASDs) with induction machines (IMs) have been making significant inroads in industry in the last decade. However, they have drawbacks due to their highly coupled nonlinear structure and the errors that occur due to parameter variations, integral drift and noise. In the last two decades some researchers have tried to overcome these problems by applying advance nonlinear control methods to these drives [10]-[12].

Among these methods, the well-known DTC strategy seems to be practically useful for IM drive systems. With the use of DTC, it is possible to obtain good dynamic control of the torque. Classical DTC presents some disadvantages that can

be summarized as: a high current and torque ripple; variable switching frequency behavior; a high noise level at low speeds; and a lack of direct current control [13].

One way to overcome the above drawbacks is with SM control combined with adaptive nonlinear techniques. The SM control objective consists of finding a suitable manifold so that the state trajectories of the plant are restricted to this manifold. Then, determine a switching control law that enforces the state trajectory to this manifold. That is, a control law is determined such that the selected manifold is made attractive and invariant.

In [14] an adaptive SM control is proposed. The controller scheme is implemented in a rotor flux field oriented reference frame. In the adaptive SM control system an adaptive algorithm is utilized to estimate the bound of the uncertainties. The main drawback of this controller is the lack of convergence of the estimated bound to its real value. Even in such adaptive scheme, the estimated bound may become very large and cause chattering. In [15] an adaptive SM control is proposed based on a real-time genetic algorithm which suffers from similar drawbacks. In addition, the controller in [15] needs more calculations. In [16] an adaptive fuzzy SM Control is introduced for IMs. The controller in [16] needs a complicated and time consuming design procedure because of the existence of a fuzzy section. In [17] a fuzzy SM control using an adaptive tuning technique is proposed for an IM. This controller is implemented in a rotor field oriented reference frame which needs a transformation from a stationary reference frame. The sliding surface used in [17] is a proportional-derivative type surface. The derivative amplifies the measurement noise in a closed-loop system.

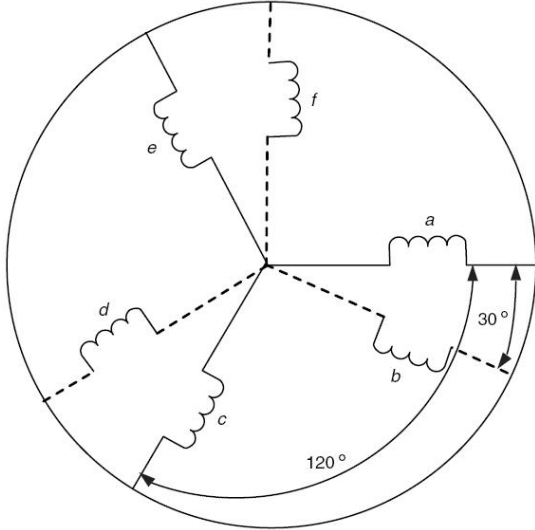A nonlinear SM torque control with a third order adaptive

Fig. 1.   Representation of a quasi six-phase (split phase, dual three-phase) machine stator winding.

backstepping approach has been presented in [18] for an IM drive system. In [18], the torque and rotor flux are controlled to track a desired linear reference model. Although the composite nonlinear controller of [18] is robust in IM stator and rotor resistance variations and uncertainties, it has some disadvantages in implementation. In fact in designing the third order adaptive backstepping controller, overparameter estimation is mandatory.

In this paper, by combining a nonlinear SM control with an adaptive input-output feedback linearization a robust nonlinear controller is proposed for IMs in general. Since the transient dynamics of the nonlinear system are difficult to evaluate by the linear control theory, like [18] the model-following control technique is utilized for the proposed control to track the designed linear reference model. This controller is utilized on a quasi six-phase IM drive.

The contributions of this paper can be summarized as follows:

A robust nonlinear controller is proposed for IMs in general to achieve: 1) an adaptive SM controller without over-parametrization 2) the robustness of nonlinear SM control on a mismatched uncertain system 3) a controller that is implemented in a stationary reference frame and where there is no need for any field oriented reference frame.

The effectiveness and capability of the proposed controller are illustrated by practical results. The proposed controller is used for a quasi six-phase IM drive.

II. DESCRIPTION AND MODELING OF THE DRIVE SYSTEM

Among the different multiphase drive solutions, one of the most interesting and widely discussed in the literature is the dual three-phase IM having two sets of three-phase windings spatially shifted by 30 electrical degrees (called a quasi-six-phase machine), which is shown in Fig. 1. The neutral points of the two windings should be better isolated for elimination of the zero sequence voltages. Fig. 2 shows such a configuration supplied from a quasi six-phase VSI.

Using the decoupling Clark's transformation, the original phase variables are correlated to new variables as $f_{\alpha\beta xy} = Cf_{abcdef}$, where C is the power-invariant transformation matrix.

$$C = \sqrt{\frac{2}{6}} \begin{array}{c} \alpha \\ \beta \\ x \\ y \\ 0+ \\ 0- \end{array} \begin{bmatrix} 1 & \cos\phi & \cos 4\phi & \cos 5\phi & \cos 8\phi & \cos 9\phi \\ 0 & \sin\phi & \sin 4\phi & \sin 5\phi & \sin 8\phi & \sin 9\phi \\ 1 & \cos 5\phi & \cos 8\phi & \cos\phi & \cos 4\phi & \cos 9\phi \\ 0 & \sin 5\phi & \sin 8\phi & \sin\phi & \sin 4\phi & \sin 9\phi \\ 1 & 0 & 1 & 0 & 1 & 0 \\ 0 & 1 & 0 & 1 & 0 & 1 \end{bmatrix} \tag{1}$$

where $\phi = \pi/6$ [19].

Fig. 3 shows the equivalent circuits of a QIM. The stator and rotor voltage equations of the machine are given as [5]:

$$\begin{cases} v_{ks} = R_s i_{ks} + \frac{d}{dt}(L_s i_{ks} + L_m i_{kr}) & \text{for } k = \alpha, \beta \\ v_{ks} = R_s i_{ks} + \frac{d}{dt}(L_{ls} i_{ks}) & \text{for } k = x, y \end{cases} \tag{2}$$

$$\begin{cases} 0 = R_r i_{\alpha r} + \omega_r(L_r i_{\beta r} + L_m i_{\beta s}) + \\ \quad \frac{d}{dt}(L_r i_{\alpha r} + L_m i_{\alpha s}) \\ 0 = R_r i_{\beta r} - \omega_r(L_r i_{\alpha r} + L_m i_{\alpha s}) + \\ \quad \frac{d}{dt}(L_r i_{\beta r} + L_m i_{\beta s}) \end{cases} \tag{3}$$

The torque equation of the machine is given by:

$$T_e = PL_m(i_{\alpha r} i_{\beta s} - i_{\beta r} i_{\alpha s}) \tag{4}$$

where P is the number of pole pairs. It can be seen that the motor (i_{xs}, i_{ys}) current components do not contribute to torque production. Moreover, it is worthwhile to note that, when the neutral points of the two windings sets of the machine are isolated, the zero sequence components ($\mathbf{0}^{\pm}$) become zero.

One can see that there is no difference in the (α, β) circuit here for a six-phase machine, when compared to the corresponding circuits of a three-phase machine. In principle, any control approach available for a three-phase machine can be used for a multi-phase machine.

III. INPUT OUTPUT FEEDBACK LINEARIZATION (IOFL) AND SM CONTROLLER

The state-coordinate transformed model of the machine is expressed by:

$$\dot{x} = f(x) + g_1 v_{\alpha s} + g_2 v_{\beta s} \tag{5}$$

where $x = \begin{bmatrix} i_{\alpha s} & i_{\beta s} & \lambda_{\alpha s} & \lambda_{\beta s} \end{bmatrix}^T$ and

$$f(x) = \begin{bmatrix} -(\frac{R_s}{\sigma L_s} + \frac{R_r}{\sigma L_r})i_{\alpha s} - \omega_r i_{\beta s} + \frac{R_r}{L_s L_r}\lambda_{\alpha s} + \frac{\omega_r}{\sigma L_s}\lambda_{\beta s} \\ -(\frac{R_s}{\sigma L_s} + \frac{R_r}{\sigma L_r})i_{\beta s} + \omega_r i_{\alpha s} + \frac{R_r}{L_s L_r}\lambda_{\beta s} - \frac{\omega_r}{\sigma L_s}\lambda_{\alpha s} \\ -R_s i_{\alpha s} \\ -R_s i_{\beta s} \end{bmatrix}$$

$$\begin{aligned} g_1 &= \begin{bmatrix} \frac{1}{\sigma L_s} & 0 & 1 & 0 \end{bmatrix}^T \\ g_2 &= \begin{bmatrix} 0 & \frac{1}{\sigma L_s} & 0 & 1 \end{bmatrix}^T \end{aligned} \tag{6}$$
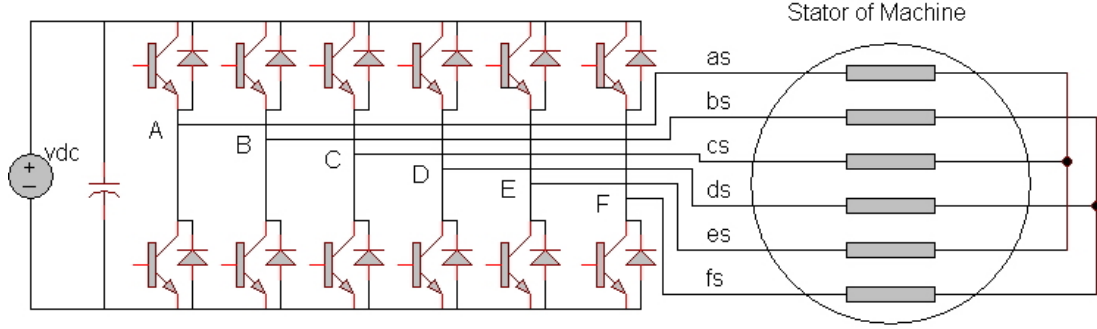
here $\sigma = 1 - L_m^2/(L_r L_s)$.

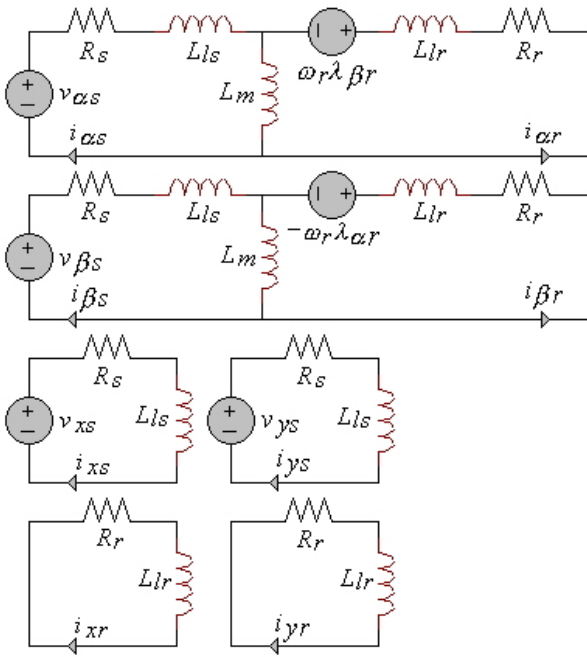Fig. 2.   A six-phase machine drive supplied by a VSI.

Fig. 3.   Equivalent circuits of the QIM.

The generated torque T_e and the squared norm of the stator flux linkage ($\lambda_s^2 = \lambda_{\alpha s}^2 + \lambda_{\beta s}^2$) are requested to be controlled output. Therefore, let:

$$h_1(x) = P(\lambda_{\alpha s} i_{\beta s} - \lambda_{\beta s} i_{\alpha s}) \qquad (7)$$
$$h_2(x) = \lambda_{\alpha s}^2 + \lambda_{\beta s}^2. \qquad (8)$$

Define the following change coordinates:

$$z_1 = h_2(x) \quad z_2 = h_1(x). \qquad (9)$$

The system model shown in (5) is reduced to:

$$\begin{bmatrix} \dot{z}_1 \\ \dot{z}_2 \end{bmatrix} = \begin{bmatrix} L_f h_2 \\ L_f h_1 \end{bmatrix} + \begin{bmatrix} 2\lambda_{\alpha s} & 2\lambda_{\beta s} \\ L_{g1}h_1 & L_{g2}h_1 \end{bmatrix} \begin{bmatrix} v_{\alpha s} \\ v_{\beta s} \end{bmatrix} \qquad (10)$$

here L_f, L_{g1} and L_{g2} are the Lie derivatives;

$$L_f h_2 = -2R_s(i_{\alpha s}\lambda_{\alpha s} + i_{\beta s}\lambda_{\beta s}),$$

$$L_{g1}h_1 = P(-\frac{1}{\sigma L_s}\lambda_{\beta s} + i_{\beta s}),$$

$$L_{g2}h_1 = P(\frac{1}{\sigma L_s}\lambda_{\alpha s} - i_{\alpha s}),$$

$$L_f h_1 = -P\lambda_{\beta s}[-(\frac{R_s}{\sigma L_s} + \frac{R_r}{\sigma L_r})i_{\alpha s} - \omega_r i_{qs} + \frac{\omega_r}{\sigma L_s}\lambda_{\beta s}]$$
$$+ P\lambda_{\alpha s}[-(\frac{R_s}{\sigma L_s} + \frac{R_r}{\sigma L_r})i_{\beta s} + \omega_r i_{\alpha s} - \frac{\omega_r}{\sigma L_s}\lambda_{\alpha s}]$$

To achieve decoupling, the following nonlinear state feedback control is employed:

$$\begin{bmatrix} \hat{v}_{\alpha s} \\ \hat{v}_{\beta s} \end{bmatrix} = \begin{bmatrix} 2\lambda_{\alpha s}v_{\alpha s} + 2\lambda_{\beta s}v_{\beta s} \\ L_{g1}h_1 v_{\alpha s} + L_{g2}h_1 v_{\beta s} \end{bmatrix} \qquad (11)$$

$\hat{v}_{\alpha s}$ and $\hat{v}_{\beta s}$ are new control inputs.

System (10) is written as:

$$\begin{bmatrix} \dot{z}_1 \\ \dot{z}_2 \end{bmatrix} = \begin{bmatrix} L_f h_2 \\ L_f h_1 \end{bmatrix} + \begin{bmatrix} \hat{v}_{\alpha s} \\ \hat{v}_{\beta s} \end{bmatrix} \qquad (12)$$

A second order linear reference model is introduced as:

$$\dot{z}_m = A_m z_m + B_m u_{ref}$$

$$\begin{bmatrix} \dot{z}_{m1} \\ \dot{z}_{m2} \end{bmatrix} = \begin{bmatrix} -a_{m1} & 0 \\ 0 & -a_{m2} \end{bmatrix} \begin{bmatrix} z_{m1} \\ z_{m2} \end{bmatrix} + \begin{bmatrix} a_{m1} & 0 \\ 0 & a_{m2} \end{bmatrix} \begin{bmatrix} \lambda_s^{*2} \\ T_e^* \end{bmatrix} \qquad (13)$$

where z_m is the output vector of the reference model; a_{m1} and a_{m2} are the positive constants.

The tracking errors between the plant and the reference model are given as:

$$e_z = \begin{bmatrix} z_1 - z_{m1} & z_2 - z_{m2} \end{bmatrix}^T = \begin{bmatrix} e_{z1} & e_{z2} \end{bmatrix}^T. \qquad (14)$$

The error dynamics are derived as follows:

$$\dot{e}_z = A(x) + \bar{V} \qquad (15)$$

where

$$A(x) = \begin{bmatrix} L_f h_2 \\ L_f h_1 \end{bmatrix}, \bar{V} = \begin{bmatrix} \bar{v}_{\alpha s} \\ \bar{v}_{\beta s} \end{bmatrix} = \begin{bmatrix} \hat{v}_{\alpha s} + a_{m1}z_{m1} - a_{m1}\lambda_s^{*2} \\ \hat{v}_{\beta s} + a_{m2}z_{m2} - a_{m2}T_e^* \end{bmatrix}$$

$\bar{v}_{\alpha s}$ and $\bar{v}_{\beta s}$ are new control inputs.

Based on (15), two independent SM switching functions are defined in the vector form

$$S(e_z) = Fe_z(x) \qquad (16)$$

where $F \in R^{2 \times 2}$ is a constant non-singular matrix.

Poles	2	R_s	2.4 Ω
R_r	4.1 Ω	L_s	385 mH
L_r	385 mH	L_m	374 mH
P_n	2 Kw	f_n	50 Hz

k_p	0.5	k_i	2
γ_1	400	γ_2	400
ρ_1	300	ρ_2	300
k_1	400	k_2	450
a_{m1}	500	a_{m2}	220

It is proven in Appendix A that the following nonlinear controller guarantees the SM reaching condition:

$$\overline{V} = -F^{-1}\left[FA(x) + Qsgn(S) + KS\right] \qquad (17)$$

where $sgn(.)$ is the sign function and:

$$Q = \begin{bmatrix} q_1 & 0 \\ 0 & q_2 \end{bmatrix}, \quad K = \begin{bmatrix} k_1 & 0 \\ 0 & k_2 \end{bmatrix}, \quad q_i, k_i > 0. \qquad (18)$$

IV. ADAPTIVE INPUT-OUTPUT SM CONTROL

When the system parameters deviate from the nominal values, especially the resistances R_r and R_s, the tracking error model (15) can be rewritten as:

$$\dot{e}_{z1} = L_f h_2(x) + \phi_1 d_1(x) + \bar{v}_{\alpha s} \qquad (19)$$

$$\dot{e}_{z2} = L_f h_1(x) + \phi_2 d_2(x) + \bar{v}_{\beta s} \qquad (20)$$

or in the compact form

$$\dot{e}_z = [A(x) + \Delta A(x)] + \bar{V} \qquad (21)$$

where ϕ_i and $\Delta A(x)$ denote uncertainties as follows:

$$[\phi_1 d_1(x) \quad \phi_2 d_2(x)]^T = \Delta A(x)$$

$$\phi_1 = 2\Delta R_s, \quad \phi_2 = P\left(\frac{\Delta R_s}{\sigma L_s} + \frac{\Delta R_r}{\sigma L_r}\right),$$

$$d_1 = -\lambda_{\alpha s} i_{\alpha s} - \lambda_{\beta s} i_{\beta s}, \quad d_2 = i_{\alpha s}\lambda_{\beta s} - i_{\beta s}\lambda_{\alpha s}$$

Since the system resistances R_r and R_s are varied with the thermal drift slowly, we assume that $|\phi_i|$ is an unknown and bounded constant.

It is proven in Appendix B that the following nonlinear controller guarantees the convergence of e_{z1} and e_{z2} to zero.

$$\dot{\hat{\phi}}_1 = \gamma_1 e_{z1} d_1 \qquad \dot{\hat{\phi}}_2 = \gamma_2 e_{z2} d_2 \qquad (22)$$

$$\begin{aligned} \bar{v}_{\alpha s} &= -L_f h_2 - \hat{\phi}_1 d_1 - k_1 e_{z1} - \rho_1 sgn(e_{z1}) \\ \bar{v}_{\beta s} &= -L_f h_1 - \hat{\phi}_2 d_2 - k_2 e_{z2} - \rho_2 sgn(e_{z2}) \end{aligned} \qquad (23)$$

here ρ_1 and ρ_2 are positive constants.

V. PRACTICAL RESULTS

The proposed control scheme is implemented in the block diagram shown in Fig. 4. The error between the reference speed and the measured speed is given to a PI controller. The output of the PI controller is considered as the reference torque. Using (11), (13), (22) and (23) the reference voltages are generated.

The stator flux estimator employed in Fig. 4 is from [20] and it is independent from the adaptive SM controller.

Practical results are obtained for a QIM with the parameters given in table I.

The parameters of the controllers are obtained by trial and error and given in table II. The first row of this table contains the PI coefficients. The experimental rig is illustrated in Fig. 5. A dual-three phase IM drive has been constructed to perform the experimental tests. The switching frequency of the six-phase IGBT inverter has been set at 4 kHz. The control software has been implemented on a PC. A Xilinx XC95288 CPLD is used for real time implementation of the switching patterns and to send the data from the A/Ds used to measure the currents and the dc-link voltage. The CPLD board communicates with the PC via a digital Advantech PCI-1751 I/O board. A second Xilinx XC95108 CPLD is used to calculate and send the speed data from an encoder to the computer through a printer port. The currents are measured using LEM sensors. The control code is written in C. The QIM is obtained by rewinding the stator of a three-phase machine.

To compare the adaptive SM controller, the SM controller and the controller with only k_i gains, two practical tests have been done with a -30% error in R_s and R_r. In the first test, the ability of the mentioned controllers is examined for direct torque control. The results of this test are shown in Fig. 6. It can be seen that for the adaptive SM controller, the torque and the flux magnitude converge to their references with a good dynamic. The results show the superiority of the adaptive SM controller.

In the second test, the speed control is examined. The results of this test are shown in Fig. 7. The errors of the speeds are shown in this figure. Using the adaptive SM controller, the speed and flux magnitude converge to their references with a better dynamic. In Fig. 7, $\hat{\phi}_1$ and $\hat{\phi}_2$ are also shown. There is no guarantee on the convergence of $\hat{\phi}_1$ and $\hat{\phi}_2$ to their real values. In the proof of the stability of the adaptive SM controller, only the convergence of the torque and flux magnitude errors to their references is proven by Barbalat lemma despite uncertainties in R_s and R_r. $\hat{\phi}_1$ and $\hat{\phi}_2$ are only bounded since the derivative of the Lyapunov function in the proof is negative semi definite. It is worthwhile to note that the aim of the proposed adaptive scheme is to achieve robustness with respect to uncertainties in R_s and R_r not estimate them.

Another test is conducted, to further verify the decoupling of the control of the torque and the stator flux as well as the capability of the proposed control scheme. Fig. 8 shows the practical results for the speed reversal of the QIM. The speed reference of the QIM is changed from 100 to -100 rad/s linearly in 1 second for $t \in [5,6]$ and the stator flux reference is kept constant at 0.4 Wb. The stator flux of the machine is shown in Fig. 8; one can observe from Fig. 8 that the stator flux amplitude remains constant during the speed reversal. The two axis $\alpha - \beta$ voltage references are also shown.
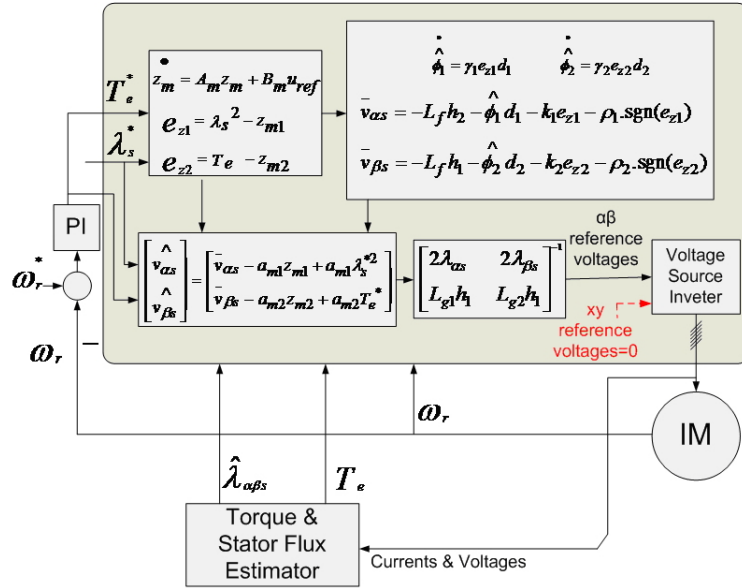
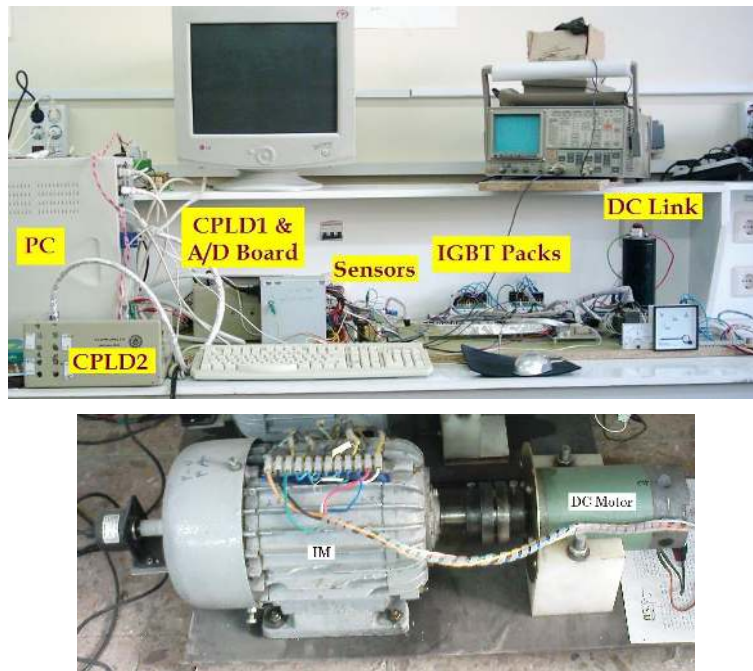Fig. 4.   Drive system block diagram.

Fig. 5.   Experimental rig: PC, CPLD boards and inverter (top), QIM (bottom).

VI. CONCLUSIONS

This paper discussed a quasi six-phase motor drive which is supplied by a six-phase VSI. An adaptive nonlinear controller has been designed that is capable of controlling the stator flux and the torque of the motor separately. The proposed controller in this paper can track the desired torque and stator flux references in spite of motor resistances mismatching. In addition, the transient dynamic of the motor stator flux and torque is precisely regulated by the design of a linear reference model, since the tracking errors between the state-transformed system and the reference model converge to zero asymptotically.

The effectiveness and validity of the proposed control method is verified by practical results. A comparison between the proposed control schemes is given by experimental tests. When using the adaptive sliding-mode controller the best tracking results are obtained.

APPENDIX A

Proof of the reachability of the SM controller:

The switching surface dynamics is:

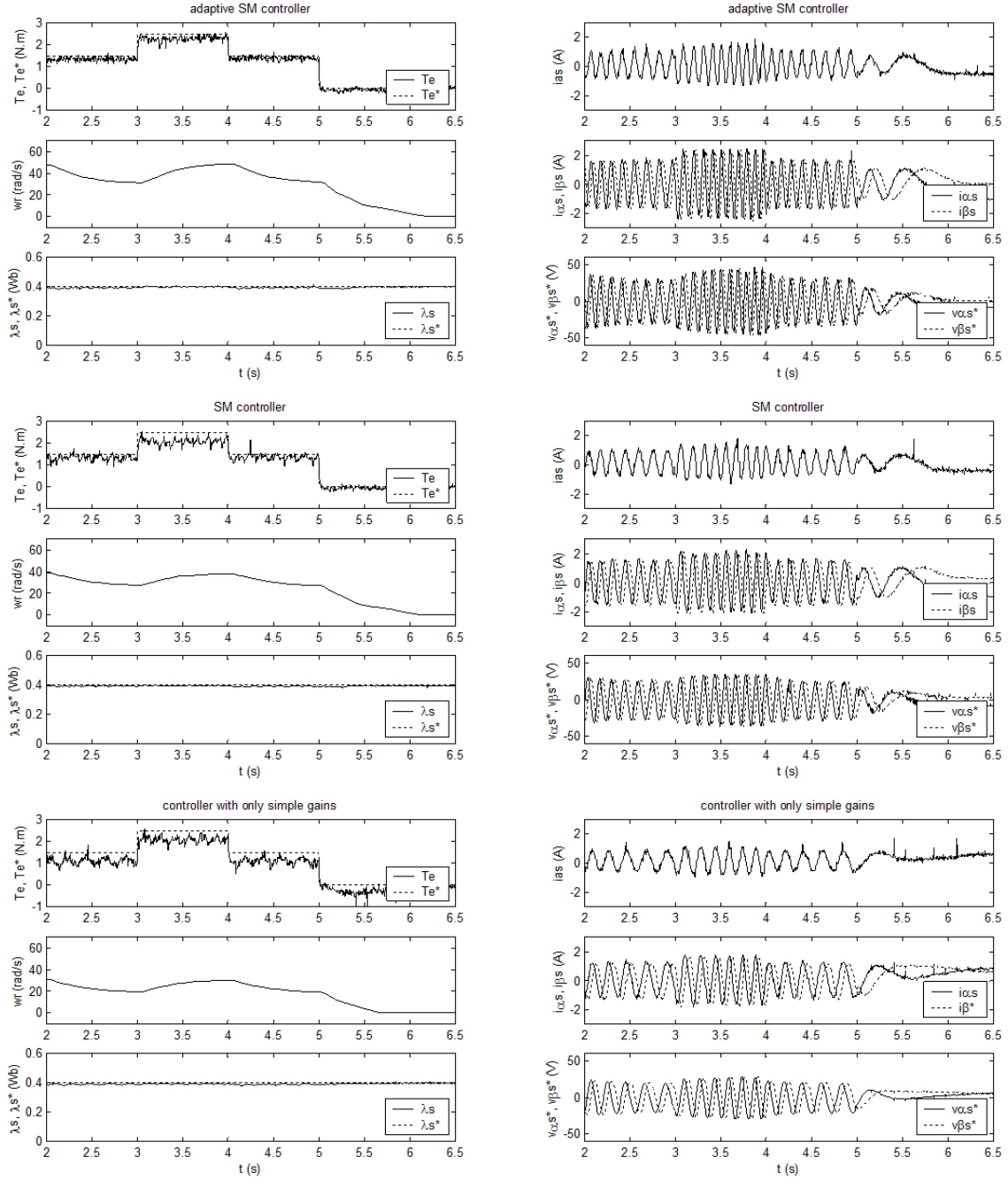$$\dot{S} = F\dot{e}_z = FA + F\overline{V} = -Q\text{sgn}(S) - KS \qquad (24)$$

Fig. 6.   Direct torque control test of the QIM.

or $\overset{\bullet}{S_i} = -q_i \text{sgn}(S_i) - k_i S_i$, $i = 1, 2$
then:

$$S_i \overset{\bullet}{S_i} = -q_i S_i \text{sgn}(S_i) - k_i S_i^2 = -q_i |S_i| - k_i S_i^2 < 0 \qquad (25)$$

Equation (25) guarantees the SM reaching condition.

APPENDIX B

Proof of the stability of the adaptive SM controller:

Choose the following Lyapunov function:

$$V = \frac{1}{2}\left\{ e_{z1}^2 + e_{z2}^2 + \frac{1}{\gamma_1}\tilde{\phi}_1^2 + \frac{1}{\gamma_2}\tilde{\phi}_2^2 \right\} \qquad (26)$$

where $\tilde{\phi}_i = \hat{\phi}_i - \phi_i$ and $\hat{\phi}_i$ is the estimate of ϕ_i and $\gamma_1, \gamma_2 > 0$ are constant gains.

Differentiating V with respect to time t one can obtain:

$$\overset{\bullet}{V} = \tilde{\phi}_1\left\{ -e_{z1}d_1 + \frac{1}{\gamma_1}\overset{\wedge\bullet}{\phi}_1 \right\} + \tilde{\phi}_2\left\{ -e_{z2}d_2 + \frac{1}{\gamma_2}\overset{\wedge\bullet}{\phi}_2 \right\} + \\ e_{z1}\left\{ L_f h_2 + \bar{v}_{\alpha s} + \hat{\phi}_1 d_1 \right\} + e_{z2}\left\{ L_f h_1 + \bar{v}_{\beta s} + \hat{\phi}_2 d_2 \right\} \qquad (27)$$

Substituting (22)-(23) into (27) one can obtain:

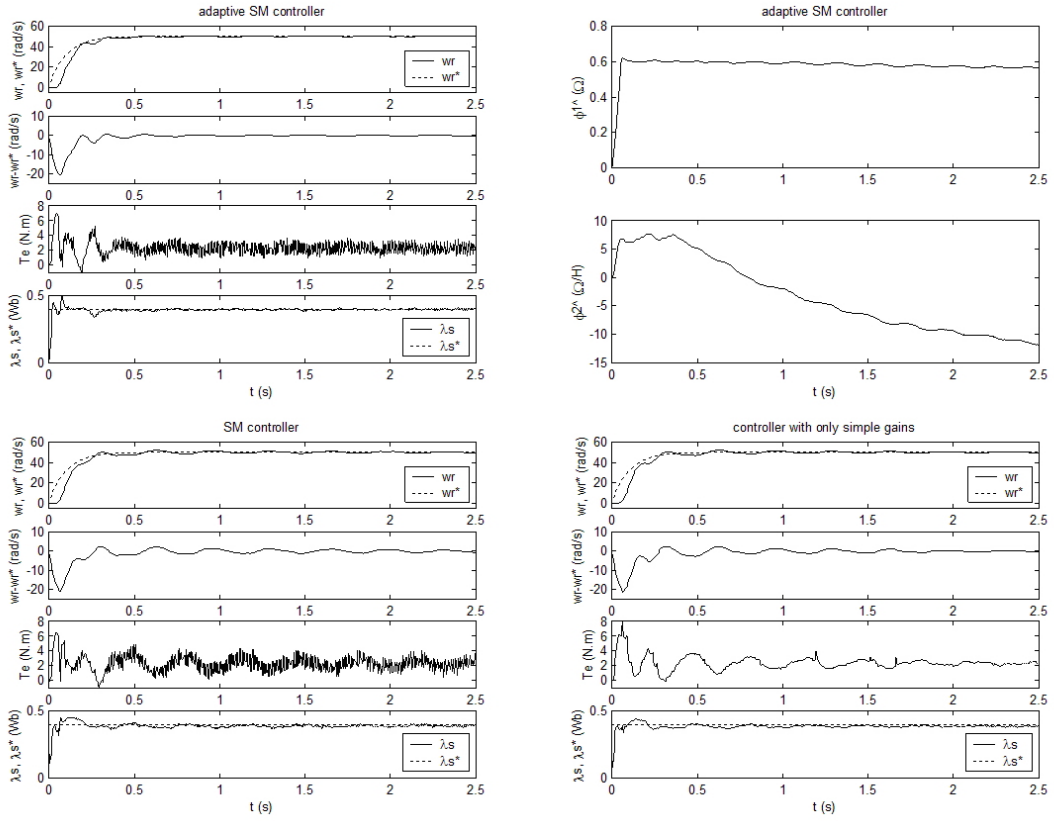$$\overset{\bullet}{V} \leq -k_1 e_{z1}^2 - k_2 e_{z2}^2 \leq 0. \qquad (28)$$
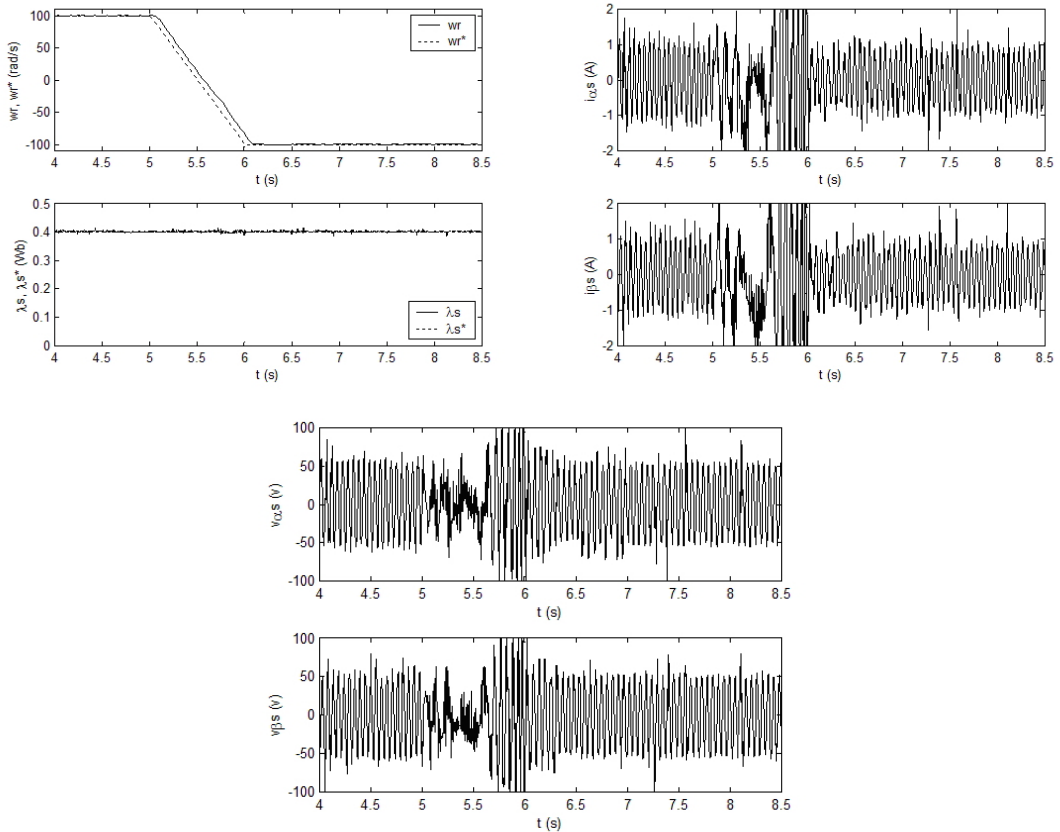
Fig. 7. Speed control test of the QIM.

Fig. 8. Speed reversal control test of the QIM using the proposed controller.

Let:

$$M(t) = k_1 e_{z1}^2 + k_2 e_{z2}^2 \geq 0. \tag{29}$$

Considering (28) and (29):

$$V(t) = V(e_z(0), \hat{\phi}(0)) + \int_0^t \dot{V}(\tau) d\tau$$
$$= V(e_z(0), \hat{\phi}(0)) - \int_0^t M(\tau) d\tau. \tag{30}$$

Since $V(t) \geq 0$ and $V(e_z(0), \hat{\phi}(0)) < \infty$, from (30), it is shown that:

$$\lim_{t \to \infty} \int_0^t M(\tau) d\tau \leq V(e_z(0), \hat{\phi}(0)) < \infty. \tag{31}$$

As a result, based on Barballat's Lemma [21]-[22]:

$$\lim_{t \to \infty} M(t) = 0 \tag{32}$$

which guarantees the convergence of e_{z1} and e_{z2} to zero if the design parameters k_1, k_2, are chosen to be positive constants.

REFERENCES

[1] E. Levi, R. Bojoi, F. Profumo, H. A. Toliyat and S. Williamson "Multiphase induction motor drives – a technology status review," *IET Electr. Power Appl.*, Vol. 1, No. 4, pp. 489˜516, Jul. 2007.

[2] L. Parsa, "On advantages of multi-phase machines," *in Proc. IECON-USA*, pp. 1574˜1579, 2005.

[3] E. Levi, D. Dujic, M. Jones, and G. Grandi "Analytical determination of DC-bus utilization limits in multiphase VSI supplied AC drives," *IEEE Trans. Energy Conv.*, Vol. 23, No. 2, pp. 433˜443, Jun. 2008.

[4] D. Dujic, G. Grandi, M. Jones, and E. Levi, "A space vector PWM scheme for multifrequency output voltage generation with multiphase voltage-source inverters," *IEEE Trans. Ind. Electron.*, Vol. 55, No. 5, pp. 1943˜1955, May 2008.

[5] R. Bojoi, E. Levi, F. Farina, A. Tenconi, and F. Profumo, "Dual three-phase induction motor drive with digital current control in the stationary reference frame," *IEE Proc.-Electr. Power Appl.*, Vol. 153, No. 1, pp. 129˜139, Jan. 2006.

[6] R. Kianinezhad, B. Nahid-Mobarakeh, L. Baghli, F. Betin, and G.-A. Capolino, "Modeling and control of six-phase symmetrical induction machine under fault condition due to open phases," *IEEE Trans. Ind. Electron.*, Vol. 55, No. 5, pp. 1966˜1977, May 2008.

[7] E. Levi, "Multiphase electric machines for variable-speed applications", *IEEE Trans. Ind. Electron.*, Vol. 55, No. 5, pp. 1893˜1909, May 2008.

[8] W.-S. Oh, S.-K. Han, S.-W. Choi, and G. W. Moon, "A three phase three-level PWM switched voltage source inverter with zero neutral point potential," *Journal of power electr.*, Vol. 5, No. 3, pp. 224˜232, Jul. 2005.

[9] M. G. Hosseini Aghdam, S. H. Fathi, and G. B. Gharehpetian, "Harmonic optimization techniques in multi-level voltage-source inverter with unequal DC sources", *Journal of power electr.*, Vol. 8, No. 2, pp. 171˜180, Apr. 2008.

[10] M. M. Salem, "Classical controller with intelligent properties for speed control of vector controlled induction motor," *Journal of Power Electronis*, Vol. 8, No. 3, pp. 210˜216, Jul. 2008.

[11] B. Castillo-Toledo, S. Di Gennaro, A. G. Loukianov, and J. Rivera, "Hybrid control of induction motors via sampled closed representations," *IEEE Tran on Ind. Electr.*, Vol. 55, No. 10, pp. 3758˜3771, Oct. 2008.

[12] S. Maiti, C. Chakraborty, Y. Hori, and M. C. Ta, "Model reference adaptive controller-based rotor resistance and speed estimation techniques for vector controlled induction motor drive utilizing reactive power," *IEEE Trans. on Ind. Electr.*, Vol. 55, No. 2, pp. 594˜601, Feb. 2008.

[13] I. Takahashi and Y. Ohmori, "High-performance direct torque control of induction motor," *IEEE Trans Ind. Appl.*, Vol. 25, No. 2, pp. 257–264, Mar./Apr. 1998.

[14] R.-J.Wai, "Adaptive sliding-mode control for induction servomotor drive," *IEE Proc.-Electr. Power Appl.*, Vol. 147, No. 6, pp. 553˜562, Nov. 2000.

[15] F.-J. Lin, W.-D. Chou, and P.-K. Huang, "Adaptive sliding-mode controller based on real-time genetic algorithm for induction motor servo drive," *IEE Proc..-EIetr. Power Appl.*, Vol. l50, No. 1, pp. 1˜13, Jan. 2003.

[16] C.-M. Lin, and C.-F. Hsu, "Adaptive fuzzy sliding-mode control for induction servomotor systems," *IEEE Trans. on Eenergy Conv.*, Vol. 19, No. 2, pp. 362˜368, Jun. 2004.

[17] R.-J. Wai, "Fuzzy sliding-mode control using adaptive tuning technique," *IEEE Trans. on Ind. Electr.*, Vol. 54, No. 1, pp. 586˜594, Feb. 2007.

[18] H.-J. Shieh, and K.-K. Shyu, "Nonlinear sliding-mode torque control with adaptive backstepping approach for induction motor drive," *IEEE Trans. on Ind. Elect.*, Vol. 46, No. 2, pp. 380˜389, Apr. 1999.

[19] Y. Zhao and T. A. Lipo, "Space vector PWM control of dual three-phase induction machine using vector space decomposition," *stocktickerIEEE Trans. on Ind. Appl.*, Vol. 31, No. 5, pp. 1100˜1109, Sep./Oct. 1995.

[20] C. Lascu, I. Boldea, and F. Blaabjerg, "Comparative study of adaptive and inherently sensorless observers for variable-speed induction-motor drives," *IEEE Trans. on Ind. Electr.*, Vol. 53, No. 1, pp. 57˜65, Feb. 2006.

[21] J. J. E. Slotine, and L. Weiping, *Applied nonlinear control,* Prentice-Hall, Inc., NJ, 1991.

[22] J. T. Spooner, *Stable Adaptive Control and Estimation for Nonlinear Systems: Neural and Fuzzy Approximator Techniques*, John Wiley and Sons Inc., NY, U.S.A., 2002.

Navid R. Abjadi was born in Isfahan, Iran. He received his B.Eng., M.Sc. and Ph.D. in Electrical Engineering from the Isfahan University of Technology, Isfahan, Iran, in 1999, 2002 and 2010, respectively. He is a lecturer at Shahrekord University. His main research interests include the application of nonlinear control and electric motor drives in general.

Gholamreza Arab Markadeh was born in Shahrekord, Iran. He graduated from the Isfahan University of Technology, Isfahan, Iran where he obtained his M.S. and Ph.D. His main areas of research interest include nonlinear control, power electronics and variable-speed ac drives.

Jafar Soltani was born in Isfahan, Iran. He graduated from Tabriz University, Tabriz, Iran. He holds a M.S. and a Ph.D. from UMIST, UK. He is a professor at the Isfahan University of Technology, Isfahan, Iran. His main areas of research include electrical machines and drives. He is a member of IEEE. He has been published in many international journal and conference papers. He also holds a UK patent.